Publications of the Astronomical Society of Australia (2025), **42**, e078, 11 pages
doi:10.1017/pasa.2025.10052

CAMBRIDGE UNIVERSITY PRESS

Research Article

Clustering and physical properties of AGN and Star-Forming Galaxies at fixed stellar mass: Does assembly bias have a role in AGN activity?

Amrita Banerjee[1], Biswajit Pandey[2], and Anindita Nandi[2]

[1]Centre for Astrophysics and Supercomputing, Swinburne University of Technology, Hawthorn, VIC, Australia and [2]Department of Physics, Visva-Bharati University, Santiniketan, West Bengal, India

Abstract

We analyse a volume-limited sample from the Sloan Digital Sky Survey to compare the spatial clustering and physical properties of active galactic nuclei (AGN) and star-forming galaxies (SFG) at fixed stellar mass. We find no statistically significant difference in clustering strength or local density between AGN and SFG. However, after matching their stellar mass distributions, we detect statistically significant differences (at a confidence level $> 99.99\%$) in colour, star formation rate (SFR), 4000Å break measurements (D4000), and morphology. These differences persist across both low- and high-density environments, suggesting that AGN are not driven by environmental factors. The development of favourable conditions for AGN activity within a galaxy may depend on the diverse evolutionary histories of galaxies. Our results imply that AGN activity may arise stochastically, modulated by the complex assembly history of galaxies.

Keywords: Methods: data analysis; methods: statistical; galaxies: statistics

(Received 13 April 2024; revised 20 May 2025; accepted 25 May 2025)

1. Introduction

AGN rank among the brightest astrophysical sources in the universe, emitting radiation across the entire electromagnetic spectrum with bolometric luminosities around $10^{47} - 10^{48}$ erg/s (Fabian, 1999; Woo and Urry, 2002). This intense radiation is believed to stem from the accretion of matter onto supermassive black holes (SMBH) located at the centers of massive galaxies. As gas clouds spiral towards the SMBH, losing angular momentum, their gravitational potential energy is converted into electromagnetic radiation (Jiang, Stone, and Davis, 2013; Cielo et al., 2018). This radiation can then heat the surrounding gas, hindering its cooling and delaying star formation (Kawata and Gibson, 2005; Antonuccio-Delogu and Silk, 2010; Wagner, Umemura, and Bicknell, 2013). Additionally, energy and momentum from AGN-driven outflows and radio jets can either heat or expel gas (Morganti, 2017; Baron et al., 2018; Santoro et al., 2020), thereby limiting black hole growth and suppressing further star formation.

AGN feedback is widely regarded as fundamental to the co-evolution of galaxies and their central black holes (Somerville et al., 2008; Kormendy and Ho, 2013; Heckman and Best, 2014; Harrison, 2017). Observations indicate a decline in the star formation rate after $z \sim 1$ (Madau et al., 1996; Hopkins, 2004; Behroozi, Wechsler, and Conroy, 2013). The observed bimodality in the colour distribution (Strateva et al., 2001; Blanton et al., 2003; Balogh et al., 2004; Baldry et al., 2004; Pandey, 2020) indicates that the galaxies are transitioning from the actively star-forming blue population to a passively evolving red sequence. The exact physical processes driving this transition, particularly the quenching of star formation in the transitional "green valley", remain uncertain (Das, Pandey, and Sarkar, 2023a). However, numerous studies propose that AGN feedback may play a crucial role in quenching star formation in this phase (Nandra et al., 2007; Hasinger, 2008; Silverman et al., 2008; Cimatti et al., 2013; Zhang et al., 2021). The models of galaxy formation and evolution increasingly rely on AGN feedback to replicate observed galaxy properties, making it an essential element in theoretical, numerical, and semi-analytic models (Springel, Di Matteo, and Hernquist, 2005; Di Matteo, Springel, and Hernquist, 2005; Eckert et al., 2021).

Nearly all massive galaxies harbour a supermassive black hole (SMBH) at their center, yet only a subset exhibit AGN activity at any given time. Understanding what triggers AGN activity in these galaxies is critical, as various internal and external factors shape the likelihood of such activity. Internal characteristics, such as gas availability in the central region, host galaxy kinematics, and morphology, significantly influence the accretion of gas onto the central SMBH (Ruffa et al., 2019; Shangguan et al., 2020; Ellison et al., 2021; Sampaio et al., 2023). Additionally, the mass of the host dark matter halo affects gas reservoir availability and the galaxy's capacity to draw gas from its surroundings. Larger halos, with deeper potential wells, facilitate gas inflow towards the galactic center, thus making AGN activity more probable (Georgakakis et al., 2019; Aird and Coil, 2021; Luo et al., 2022). Observational data also reveal that AGN activity is more frequent in massive galaxies (Dunlop et al., 2003; Brusa et al., 2009; Pimbblet et al., 2013).

The SMBH mass itself plays a vital role in AGN dynamics. The larger black holes exert stronger gravitational forces, enabling higher accretion rates and boosting AGN luminosity. Meanwhile, AGN feedback can limit black hole growth by modulating gas supply. Massive galaxies, often found in high-mass dark matter halos

Author for correspondence: Biswajit Pandey, Email: biswap@visva-bharati.ac.in.

Cite this article: Banerjee A, Pandey B and Nandi A. (2025) Clustering and physical properties of AGN and Star-Forming Galaxies at fixed stellar mass: Does assembly bias have a role in AGN activity?. *Publications of the Astronomical Society of Australia* **42**, e078, 1–11. https://doi.org/10.1017/pasa.2025.10052

within dense environments like galaxy clusters and cosmic web filaments, may experience indirect influence from these environments. Observations suggest that galaxy colour and star formation rates are sensitive to cosmic web environments (Pandey and Sarkar, 2020; Das, Pandey, and Sarkar, 2023b,c). Furthermore, gas inflow along cosmic web filaments can initiate and sustain AGN activity within galaxies (Umehata et al., 2019).

Numerous studies indicate that AGN are more strongly clustered than SFG (Gilli et al., 2009; Mandelbaum et al., 2009; Kollatschny, Reichstein, and Zetzl, 2012; Donoso et al., 2014; Hale et al., 2018). Using SDSS data, Satyapal et al. (2014) observe that the fraction of AGN increases as the distance to neighbouring galaxies decreases. Similarly, Zhang et al. (2021) find that AGN have more neighbouring galaxies compared to SFG. Results from the Horizon Run 5 simulation (Lee et al., 2021), as analysed by Singh et al. (2023), show that AGN activity rises in response to both higher background densities and closer proximity to neighbouring galaxies. Physical mechanisms, including major and minor mergers (Di Matteo, Springel, and Hernquist, 2005; Alonso et al., 2007; Ellison et al., 2011; Storchi-Bergmann and Schnorr-Müller, 2019), disk instability (Hopkins and Hernquist, 2006; Dekel, Sari, and Ceverino, 2009; Hopkins, Kocevski, and Bundy, 2014), and tidal effects (Moore et al., 1996), are thought to enhance the supply of cold gas to the central SMBH, thereby boosting AGN activity. Interactions and mergers, more common in clusters and filaments, often drive gas inflows towards galactic centers, further promoting AGN activity (Hernquist, 1989; Springel, Di Matteo, and Hernquist, 2005; Alexander and Hickox, 2012).

While AGN are generally more common in dense environments, extremely high-density regions like massive galaxy clusters present a more complex picture. The pressure from the hot intracluster medium (ICM) at the centers of massive galaxy clusters can cause ram pressure stripping of the cold gas that fuels the AGN activity (Gunn and Gott, 1972; Abadi, Moore, and Bower, 1999; Boselli, Fossati, and Sun, 2022). Additionally, the cluster halo may capture the cold gas, preventing accretion towards the inner regions by strangulation (Larson, Tinsley, and Caldwell, 1980; Peng, Maiolino, and Cochrane, 2015). These processes often suppress AGN activity near the centers of massive galaxy clusters. Ehlert et al. (2014) observe that the fraction of X-ray bright AGN rises with increasing distance from the centers of galaxy clusters, and Lopes, Ribeiro, and Rembold (2017) find that AGN are more frequently located in low-mass groups, field environments, and cluster outskirts. The XXL survey (Pierre et al., 2016), as analysed by Koulouridis et al. (2018), reveals that the relationship between X-ray-selected AGN and environment differs between high- and low-mass clusters. Studies of X-ray selected clusters from ROSAT by Mishra and Dai (2020) show a lower AGN fraction in clusters compared to fields, while Ceccarelli, Duplancic, and Garcia Lambas (2021) find AGN activity significantly stronger in voids compared to field environments.

Low-density regions, such as voids, tend to host less evolved galaxies due to the lack of external processes, like gas stripping and frequent mergers, and contain large reservoirs of pristine gas. Galaxies in these environments evolve through internal, or secular, processes and are typically fainter, bluer, and exhibit higher star formation rates than galaxies in average-density environments (Grogin and Geller, 2000; Hoyle et al., 2005; Ricciardelli et al., 2014; Bruton et al., 2020). Constantin, Hoyle, and Vogeley (2008) find that moderately luminous AGN are more common in voids than walls, but the abundance of brighter AGN are comparable in the two environments. Kauffmann, Heckman, Tremonti, et al. (2003) observe a decreasing AGN fraction in massive galaxies as density increases, and several other works report a higher prevalence of AGN in low- to moderate-density environments (Kauffmann et al., 2004; Gilmour et al., 2007; Choi, Woo, and Park, 2009; Sabater, Best, and Argudo-Fernández, 2013; Miraghaei, 2020; Mishra, Dai, and Guerras, 2021). This trend suggests that galaxies in voids may experience a higher frequency of one-on-one interactions, which may be key to triggering AGN activity in these regions.

The environmental dependence of AGN activity at higher redshifts has been investigated in several studies. Using data from the zCOSMOS spectroscopic survey up to $z \sim 1$, Silverman et al. (2009) find that massive galaxies hosting AGN tend to reside in low-density regions. In contrast, Bradshaw et al. (2011) analyse the UKIDSS Ultra-deep Survey in the redshift range $z \sim 1 - 1.5$ and observe that AGN are more frequently found in high-density environments. More recent studies provide growing evidence for a positive evolution of AGN activity with redshift, particularly in dense environments such as galaxy clusters. Several works have demonstrated that the fraction of AGN in clusters increases with redshift, implying a stronger connection between environment and AGN triggering at earlier times (Fassbender, Šuhada, and Nastasi, 2012; Martini et al., 2013; Bufanda et al., 2017; Hashiguchi et al., 2023). Numerous studies also reported a high incidence of AGN in proto-cluster environments, further supporting the idea that dense regions at high redshift are conducive to AGN activity (Lehmer et al., 2013; Krishnan et al., 2017; Gatica et al., 2024; Vito et al., 2024).

Several other studies suggest that AGN activity shows little to no dependence on environmental factors. Miller et al. (2003) report that the fraction of optically selected AGN remains consistent from the cores of galaxy clusters to field regions, a finding mirrored by Martini, Mulchaey, and Kelson (2007) for X-ray-selected AGN. Similarly, Pandey and Bharadwaj (2008) analyse SDSS data, comparing filamentarity in the distributions of SFG and AGN, and find no significant difference. Pimbblet et al. (2013) observe that the fraction of optically selected AGN does not vary with distance from the cluster center, while Sabater, Best, and Heckman (2015) find no statistically significant effect of environment on optical AGN activity. Likewise, Amiri, Tavasoli, and De Zotti (2019) report only a weak correlation between local galaxy density and AGN activity, and Man et al. (2019), analyzing SDSS data, find minimal to no environmental influence on AGN occurrence. Some studies find no significant differences in the clustering of AGN and non-AGN galaxies (Porqueres et al., 2018; Wang and Li, 2019). These apparently conflicting results suggest that the role of environment in AGN activity remains an open question, underscoring the need for further research to resolve the uncertainties.

The SDSS (Stoughton et al., 2002) provides high-quality spectra and imaging for a large number galaxies in the nearby universe, making it one of the largest and most comprehensive redshift surveys to date. The precise classification of SFG and AGN based on emission lines enables a robust statistical comparison between these populations. In this study, we investigate the clustering properties of SFG and AGN using statistical tools such as the two-point correlation function and nearest neighbour distribution. The mass of a galaxy is known to influence the AGN activity. However, galaxy mass is known to depend on environment. To identify any additional dependence of AGN activity on the environment,

https://doi.org/10.1017/pasa.2025.10052 Published online by Cambridge University Press

we will compare the spatial clustering and physical properties of the SFG and AGN after matching their stellar mass distributions. This approach will allow us to assess any residual environmental impact on AGN activity by comparing the spatial clustering and physical properties of SFG and AGN at similar masses across varying densities. Additionally, analyzing AGN and SFG properties in different environments at the same mass could clarify the influence of large-scale environment and assembly bias (Gao, Springel, and White, 2005; Wechsler et al., 2006; Gao and White, 2007; Croton, Gao, and White, 2007). The dark matter halos of similar mass may have distinct assembly histories leading to different halo concentration, merger rates, or gas accretion rates, potentially impacting the AGN activity. In this study, we will explore the possible roles of assembly bias on the AGN activity in galaxies.

We use a ΛCDM cosmological model with $\Omega_{m0} = 0.315$, $\Omega_{\Lambda 0} = 0.685$ and $h = 0.674$ (Planck Collaboration et al., 2020) throughout the present work.

The outline of our work is as follows. In Section 2, we describe our data and the methods of analysis. Section 3 presents our results, and in Section 4, we provide our conclusions.

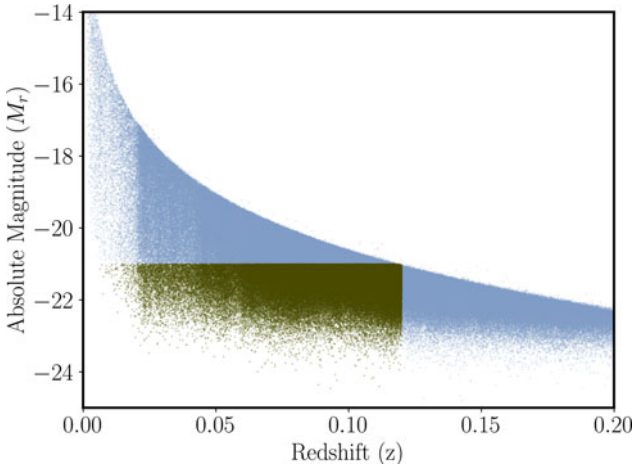

Figure 1. This shows the definition of the volume limited sample in the redshift-absolute magnitude plane. The volume limited sample comprises of the galaxies lying within the rectangular region in this diagram.

2. Data and method of analysis

2.1 SDSS data

We use data from the 17^{th} data release (DR17) of SDSS (Abdurro'uf et al. (2022), which is a multi-band imaging and spectroscopic redshift survey. The SDSS employs a 2.5 m optical telescope (Gunn et al., 2006) at Apache Point Observatory in New Mexico, USA, to gather photometric and spectroscopic data on galaxies across one-quarter of the entire sky. DR17 covers 14555 square degrees and includes spectroscopic information for 2863635 galaxies. For our analysis, we focus on the Main Galaxy Sample (Strauss et al., 2002) of the SDSS. The data are accessed via the SDSS CasJobs service[a] using Structured Query Language (SQL).

We select a contiguous region of the sky in equatorial coordinates, specifically the area spanning $130° \leq \alpha \leq 230°$ and $0° \leq \delta \leq 60°$, for our analysis. From this region, we download the spectroscopic data for galaxies with redshifts in the range $0 \leq z \leq 0.2$ and r-band apparent Petrosian magnitudes $m_r < 17.77$. These criteria yield a total of 392292 galaxies.

We use the *galSpecExtra* table, which is derived from the MPA-JHU spectroscopic catalog of galaxies[b], to classify the objects as AGN or SFG based on the BPT diagram (Brinchmann et al., 2004). In this table, SFG are flagged with a value of 1, while AGN are flagged with a value of 4. Our AGN sample primarily consists of high signal-to-noise ratio (SNR) narrow line AGN excluding the composite galaxies (flag 3) and galaxies with low-ionisation nuclear emission-line regions (LINERs). The information about the stellar mass and SFR are also provided in the *galSpecExtra* table. The stellar masses of the galaxies are estimated using the methodology outlined in Kauffmann, Heckman, Tremonti, et al. (2003), applied to photometric data as detailed in Salim et al. (2007). Star formation rates are calculated according to the approach discussed in Brinchmann et al. (2004). The aperture corrections are made by estimating star formation rates from SED fits to the photometry outside the fiber, following the methodology described in Salim et al. (2007). Estmating SFR in AGN through model fitting gives unreliable results since different lines are affected by AGN in different ways. The sSFR for AGN in MPA-JHU catalogue are calculated using D4000 values. The D4000, which indicate the mean age of the stellar population in galaxies (Balogh et al., 1999), are retrieved from the *galSpecIndx* table. To characterise the morphology of galaxies, we use the concentration index, $\frac{r_{90}}{r_{50}}$ Shimasaku et al. (2001), where r_{90} and r_{50} represent the radii that contain 90% and 50% of the Petrosian flux, respectively. These values are obtained from the *PhotoObjAll* table.

We construct a volume-limited sample by applying a cut on the K-corrected and extinction-corrected r-band absolute magnitude, selecting galaxies with $M_r \leq -21$. This corresponds to a redshift cut of $z \leq 0.12$. The resulting sample consists of a total of 111671 galaxies (Figure 1), which include 38606 unclassified galaxies, 17282 star-forming galaxies, 22943 low SNR star-forming galaxies, 10028 composite galaxies, 5828 AGNs, and 16984 low SNR LINERs.

We extract the largest cube that can be fitted within the volume-limited sample. This datacube has a side length of 267.5 Mpc and contains a total of 30860 galaxies, of which 5184 are SFG and 1883 are AGN. The primary objective of this work is to compare the spatial clustering and physical properties of AGN and SFG. Therefore, we focus our analysis on these two galaxy types. The spatial distributions of AGN and SFG within the extracted datacube are shown in Figure 2.

2.2 Methods of analysis

2.2.1 Matching the stellar mass distributions of the AGN and SFG

The stellar mass of a galaxy is a key factor influencing the onset of AGN activity. AGN abundance tends to increase with the stellar mass of the host galaxy (Kauffmann, Heckman, Tremonti, et al., 2003; Silverman et al., 2009). This strong correlation between AGN activity and galaxy mass could introduce significant bias into our study if not properly accounted for. To address this, we match the stellar mass distributions of AGN and SFG in our sample

[a] https://skyserver.sdss.org/casjobs/
[b] https://www.sdss4.org/dr17/spectro/galaxy_mpajhu/

https://doi.org/10.1017/pasa.2025.10052 Published online by Cambridge University Press

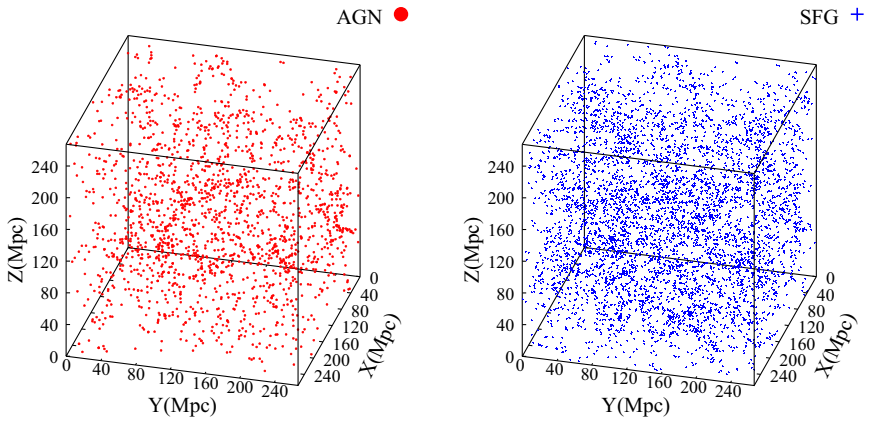

Figure 2. The left and right panels of this figure, respectively show the spatial distributions of the AGN and SFG within the datacube extracted from the volume limited sample.

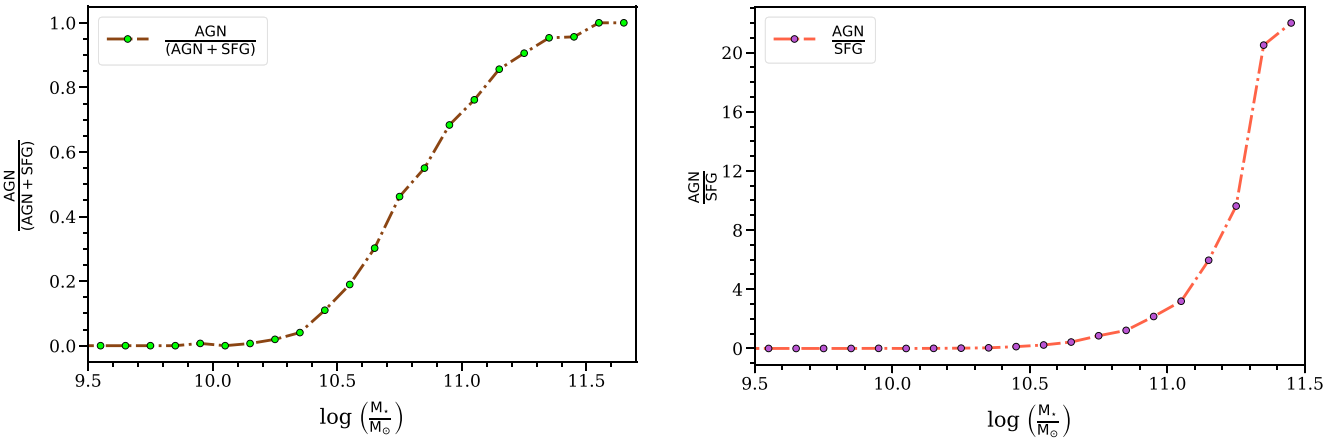

Figure 3. The left panel shows the fraction $\frac{AGN}{AGN+SFG}$ and the right panel shows $\frac{AGN}{SFG}$ as a function of stellar mass.

using the criterion $|\frac{m_{SFG}}{m_{AGN}} - 1| < 10^{-3}$. The stellar mass distributions for both AGN and SFG, before and after matching, are shown in the left and right panels of Figure 4, respectively. We apply a Kolmogorov-Smirnov (KS) test to compare the distributions after matching and find that the null hypothesis can be rejected with very low confidence (p-value $< 1\%$).

We calculate the fraction of AGN as a function of stellar mass for the galaxies in our datacube and present the results in Figure 3. The left panel of Figure 3 shows that the AGN fraction $\frac{AGN}{AGN+SFG}$ increases steadily with stellar mass for galaxies with masses greater than $\sim 10^{10.5}\,M_{\odot}$. The sharp rise in the ratio $\frac{AGN}{SFG}$ at higher masses, shown in the right panel of Figure 3, is due to the lower abundance of SFG at these mass scales. Galaxies with masses above $3 \times 10^{10}\,M_{\odot}$ are predominantly quiescent, bulge-dominated galaxies, while those with lower masses are typically actively star-forming and have disk-like morphologies (Kauffmann, Heckman, Tremonti, et al., 2003). Hydrodynamical simulations suggest that a transition occurs around this critical mass from cold-mode to hot-mode accretion, leading to mass quenching in galaxies (Birnboim and Dekel, 2003; Dekel and Birnboim, 2006; Kereš et al., 2005; Gabor et al., 2010). In these more massive galaxies, the halo gas can eventually cool and collapse to form stars. However, AGN feedback can provide additional heating, preventing this cooling and maintaining a hot halo (Fabian, 2012; McNamara and Nulsen, 2012). The higher AGN fraction observed in more massive galaxies suggests that these galaxies provide a more conducive environment for AGN activity. Moreover, the more massive galaxies are strongly clustered and tend to reside in high-density regions. This implies that any comparison of clustering between SFG and AGN would be influenced by the mass dependence of clustering.

The primary goal of this study is to compare the clustering and physical properties of SFG and AGN with similar stellar masses. Since the environment, clustering, and physical properties of galaxies are strongly influenced by its mass, we match the stellar mass distributions of the two populations to ensure that our results are not biased by mass-dependent factors. Although only about 20% of the most massive galaxies in our SFG sample are available for comparison with AGN, this approach allows us to explore the roles of other potential factors, beyond stellar mass, that might contribute to AGN activity.

2.2.2 *Two-point correlation function*

The two-point correlation function quantifies the strength of galaxy clustering at a given scale by measuring the excess

https://doi.org/10.1017/pasa.2025.10052 Published online by Cambridge University Press

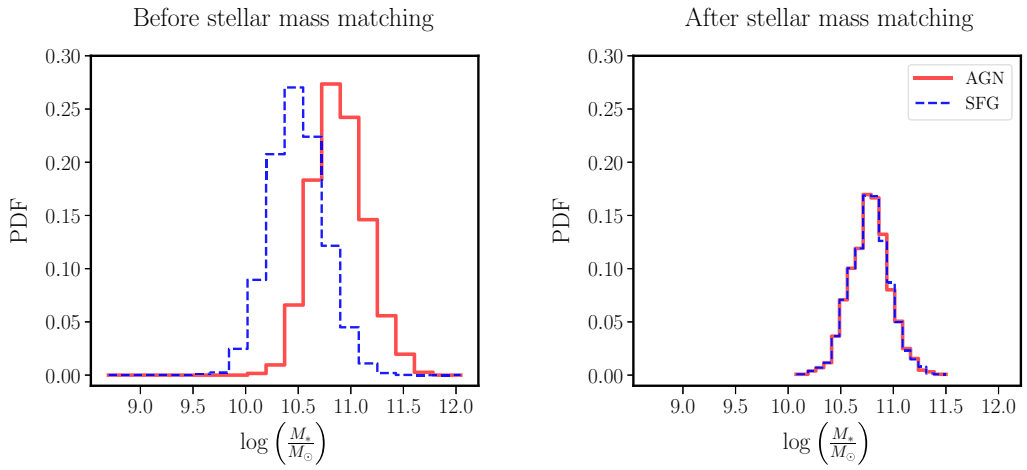

Figure 4. The left panel of this figure shows the stellar mass distributions of the AGN and SFG. We match the AGN and SFG stellar mass distributions, which are shown together in the right panel.

probability of finding two galaxies at a specific separation, compared to a random Poisson distribution. We calculate the two-point correlation function separately for the AGN and SFG samples, after matching their stellar mass distributions. The data extracted from the volume-limited sample include 1883 AGN and 5184 SFG. After stellar mass matching, we obtain 1285 AGN and 1285 SFG galaxies.

The two-point correlation function is computed using the Landy and Szalay estimator (Landy and Szalay, 1993):

$$\xi(r) = \frac{DD(r) - 2DR(r) + RR(r)}{RR(r)}, \tag{1}$$

where $DD(r)$, $RR(r)$ and $DR(r)$ are normalised counts for data-data, random-random and data-random pairs at separation r. To estimate the error bars, we generate 50 jackknife resamplings for each dataset.

2.2.3 Distribution of the n^{th} nearest neighbour distance and the local density

Galaxies in denser environments are expected to have closer neighbours. The distance to the n^{th} nearest neighbour, r_n, can serve as a proxy for the local environment (Casertano and Hut, 1985) of a galaxy, with n representing the number of neighbours considered. In our analysis, we focus on three-dimensional space and select $n = 5$ for the present study.

We calculate the distribution of the 5^{th} nearest neighbour distances for both AGN and SFG galaxies, using all 30860 galaxies in our dataset.

The local galaxy density around an AGN or SFG is defined as,

$$\eta_n = \frac{n-1}{V(r_n)}, \tag{2}$$

where, $V(r_n) = \frac{4}{3}\pi r_n^3$ is the volume within a radius r_n.

Due to the sharp boundaries of our samples, the local density can be underestimated near the edges. To address this, we calculate the minimum distance r_b from each galaxy to the boundary of the sample and only include galaxies for which $r_n < r_b$ in our local density calculations.

3. Results and discussions

3.1 The two-point correlation function and the 5^{th} nearest neighbour distribution of the mass-matched AGN and SFG

In the top-left and top-right panels of Figure 5, we show the two-point correlation function and the probability density function (PDF) of the 5^{th} nearest neighbour distance for the mass-matched AGN and SFG populations, respectively. The bottom left panel of Figure 5 reveals that AGN are somewhat more strongly clustered than SFG at fixed stellar mass. However, the statistical significance of these differences are not strong enough to confirm the differences in their clustering strength. We also repeat our calculations for the two-point correlation functions of AGN and SFG using the publicly available code *Corrfunc* (Sinha and Garrison, 2020) and obtained the same results as presented in this work.

The two-point correlation functions for AGN and SFG are analysed in redshift space, where a power-law fit provides a reasonable approximation on scales below 25 Mpc (Hawkins et al., 2003). We fit the two-point correlation functions to a power law of the form $\xi(r) = (\frac{r}{r_0})^{-\gamma}$ using least squares fitting and present the fitted values for the correlation length (r_0) and slope (γ) in Table 1. The results show that the two-point correlation function of AGN has a larger correlation length and a shallower slope compared to SFG, even after matching their stellar mass distributions. However, the errors associated with these parameters (see Table 1) suggest that r_0 and γ for AGN are consistent with SFG within 1σ.

The bottom-right panel of Figure 5 compares the 5^{th} nearest neighbour distributions for AGN and SFG using a KS test. The KS test shows that the null hypothesis can be rejected at the 95% confidence level. The distance to the 5^{th} nearest neighbour is smaller for AGNs than for SFGs, indicating that AGN are hosted in relatively higher-density regions compared to SFG. However, the significance of these differences are not sufficiently strong that can unambiguously provide an evidence in favour of a stronger clustering of AGN compared to SFG. Several earlier studies reported a stronger clustering for AGN (Gilli et al., 2009; Mandelbaum et al., 2009; Kollatschny, Reichstein, and Zetzl, 2012; Donoso et al., 2014; Hale et al., 2018). Further investigations with larger datasets are

https://doi.org/10.1017/pasa.2025.10052 Published online by Cambridge University Press

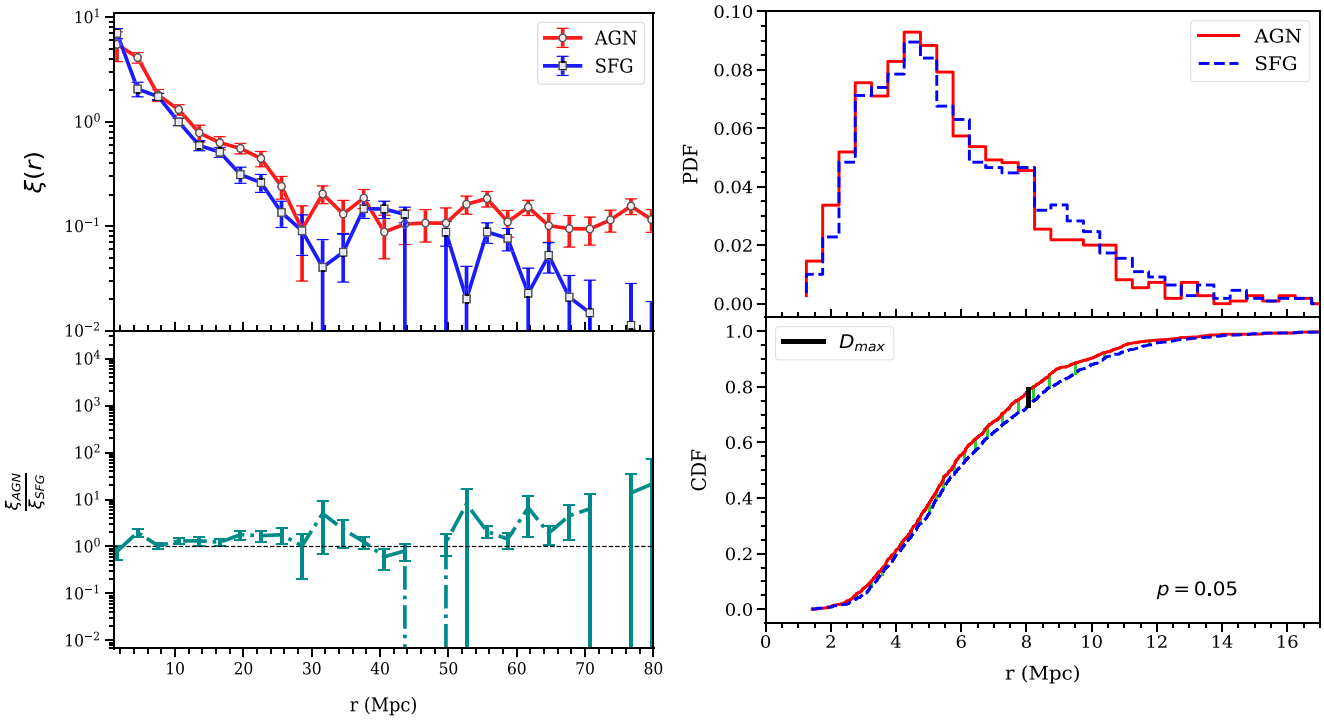

Figure 5. The top left panel of this figure shows the two-point correlation function as a function of length scale (r) for the AGN and SFG. The ratio of the two-point correlation functions for AGN and SFG is plotted as a function of r in the bottom left panel. The 1σ errorbars in these figures are obtained from 50 jackknife samples drawn from the original dataset. The top right panel shows the PDFs of the 5^{th} nearest neighbour distance for AGN and SFG. The two distributions are compared using a KS test, and the results are shown in the bottom right panel. The comparisons are carried out after matching the stellar mass distributions of AGN and SFG.

Table 1. This table shows the best fit values of r_0 and γ for the two-point correlation functions of AGN and SFG. The two-point correlation functions are fitted to a power law of the form $(\frac{r}{r_0})^{-\gamma}$ upto a scale of ~25 Mpc.

Class	Correlation length (r_0)	Slope (γ)
AGN	$r_0 = 10.82 \pm 3.41$	$\gamma = 1.09 \pm 0.13$
SFG	$r_0 = 8.36 \pm 2.57$	$\gamma = 1.29 \pm 0.12$

necessary to confirm the differences in the clustering of AGN host galaxies and star-forming galaxies at fixed stellar mass.

3.2 Comparing the distributions of different physical properties of the mass-matched AGN and SFG

The triggering of AGN activity may require specific physical conditions within a galaxy, and the onset of AGN activity can, in turn, affect certain physical properties of the host galaxy. Understanding the differences between the physical properties of AGN host galaxies and star-forming galaxies is crucial. The mass of a galaxy is known to be the most influential factor in determining its physical properties (Cooray and Sheth, 2002). Moreover, the AGN fraction is strongly correlated with the stellar mass of galaxies (Figure 3). It is therefore of interest to compare the distributions of various physical properties for the two populations after matching their stellar mass distributions.

We compare the distributions of the $(u-r)$ colour, concentration index ($\frac{r_{90}}{r_{50}}$), SFR, and the D4000 for AGN host galaxies and star-forming galaxies at fixed stellar mass. These distributions are shown in different panels of Figure 6. To quantify the dissimilarity between the two distributions in each case, we apply the KS test. The results indicate that the null hypothesis can be rejected with a confidence level greater than 99.99% in all cases.

The different panels of Figure 6 show that the PDFs for AGN and SFG cover similar ranges but peak at different values. In the top-left panel of Figure 6, we observe that most SFG are located in the blue cloud ($(u-r) < 2.22$) (Strateva et al., 2001), while the colour distribution of AGN host galaxies peaks in the green valley and extends into both the blue cloud and the red sequence.

The blue colours of SFG are primarily due to the presence of young, hot, and massive stars that dominate the emission from the galaxy. These stars emit substantial ultraviolet and blue light, giving SFG their characteristic blue colour. In contrast, AGN tend to have redder colours, which can be attributed to the dust and gas surrounding the central black hole. This dust absorbs and scatters the blue and ultraviolet light emitted by the accretion disk, causing the galaxy to appear redder. Additionally, the redder colours may result from the thermal emission of dust heated by the radiation, contributing to the infrared part of the spectrum. An older stellar population in AGN host galaxies can also contribute to their redder appearance.

We compare the SFR distributions of AGN and SFG in the top-right panel of Figure 6. The SFR distributions for SFG and AGN peak around $\sim 4\,M_{\odot}$/yr and $\sim 1\,M_{\odot}$/ yr, respectively. Both distributions are positively skewed and extend to higher SFRs (up to $15\,M_{\odot}$/yr). However, the abundance of AGN decreases significantly compared to SFG for SFRs above $3\,M_{\odot}$/yr.

The bottom-left panel of Figure 6 shows the distributions of the 4000Å break measurements for AGN and SFG. The 4000Å break is strongly correlated with the ratio of the past average SFR

https://doi.org/10.1017/pasa.2025.10052 Published online by Cambridge University Press

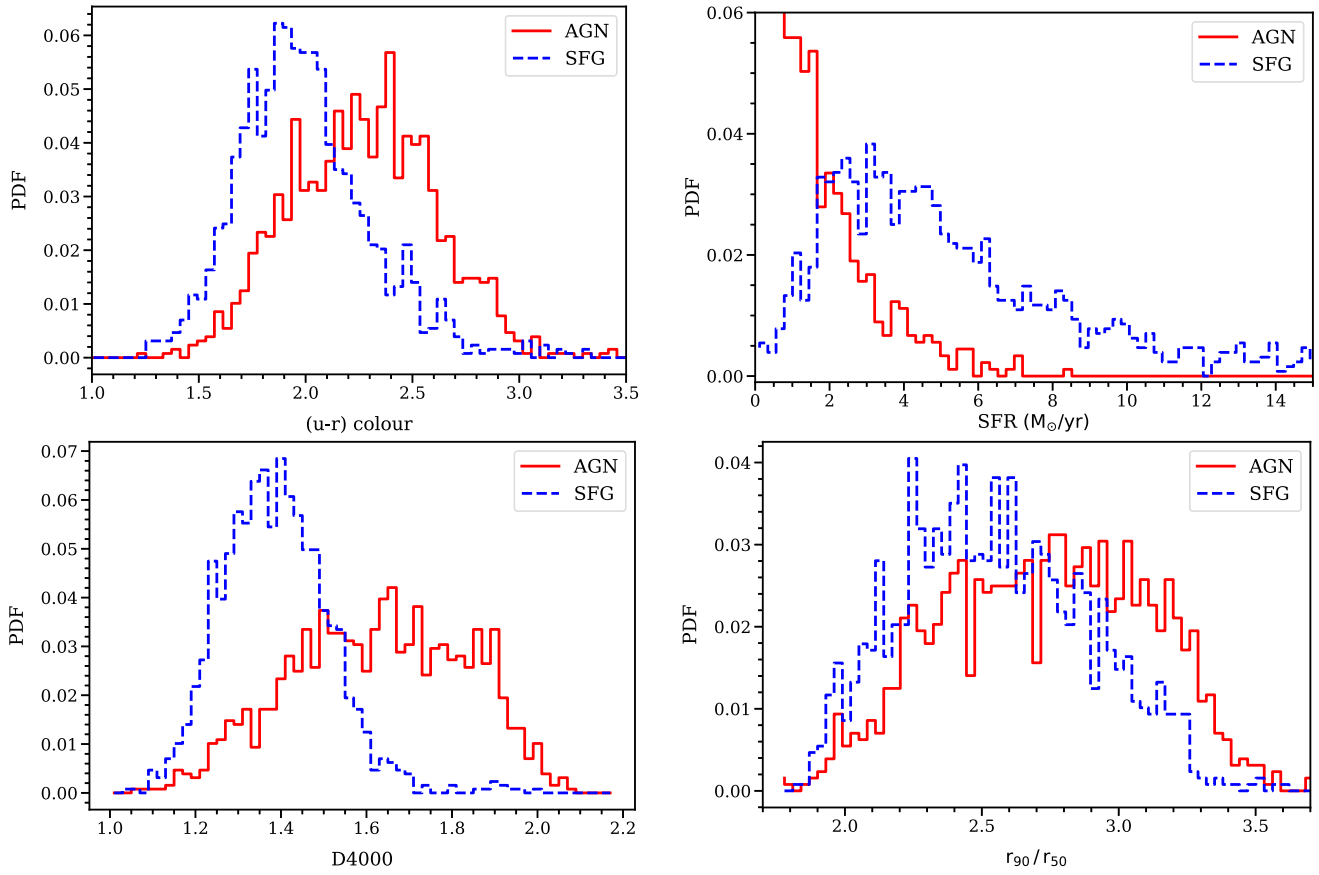

Figure 6. The different panels of this figure show the distributions of the $(u-r)$ colour, SFR, D4000 and $\frac{r_{90}}{r_{50}}$ for the AGN and SFG after matching their stellar mass distributions. We use KS-test to compare the distributions for the AGN and SFG in each case. The corresponding p-values are extremely small, and the null hypothesis can be rejected at $>$ 99.99% confidence level in each case.

to the present SFR in galaxies (Kauffmann, Heckman, Tremonti, et al., 2003), and it serves as an indicator of the galaxy's recent star formation history. The distribution for AGN peaks at a higher value of D4000 ($\sim$ 1.63) and is negatively skewed, while the distribution for SFG peaks around $\sim$ 1.38 and is nearly symmetrical. Lower values of D4000 ($<$ 1.5) are associated with younger stellar populations, indicating recent star formation or a completed starburst. Conversely, higher values ($>$ 1.8) correspond to older stellar populations (Kauffmann and Heckman, 2009). The higher D4000 values for AGN suggest that their host galaxies are primarily composed of older stellar populations. However, we also observe that some AGN host galaxies exhibit D4000 values below 1.5, implying that AGN activity can coexist with starburst activity in certain galaxies.

We compare the distributions of the concentration index for AGN and SFG in the bottom right panel of Figure 6. The concentration index is strongly correlated with galaxy morphology (Shimasaku et al. (2001). A concentration index of $\frac{r_{90}}{r_{50}} = 2.3$ corresponds to a pure exponential profile (Strateva et al., 2001), while $\frac{r_{90}}{r_{50}} = 3.33$ describes a pure de Vaucouleurs profile (Blanton et al., 2001). Higher values of the concentration index are typically associated with elliptical and bulge-dominated galaxies, whereas disk-dominated spiral galaxies have lower concentration indices ($<$ 2.6) (Strateva et al., 2001). For our sample, the concentration index distributions for AGN and SFG peak at around $\sim$ 2.8 and $\sim$ 2.3, respectively. This suggests that most SFG have disk-like morphologies, while AGN are more commonly found in bulge-dominated systems. We also note that the distribution for AGN is negatively skewed, whereas the distribution for SFG is positively skewed. This indicates that AGN can also occur in disk-dominated galaxies, and some SFG may exhibit bulge-dominated morphologies. These findings are consistent with previous studies showing that barred spiral galaxies in groups often display AGN activity (Alonso, Coldwell, and Lambas, 2014), and that some elliptical galaxies can undergo rejuvenation in isolated environments (Zezas et al., 2003; Lacerna et al., 2016).

3.3 Comparing the distributions of different physical properties of the mass-matched AGN and SFG in low and high density regions

Figure 6 shows that the physical properties of AGN and SFG differ significantly at fixed stellar masses. Analysis of the two-point correlation function and the distribution of the 5^{th} nearest neighbours (Figure 5) also reveals that AGN exhibit moderately stronger clustering than SFG. AGN tend to prefer denser regions, while SFG are more commonly found in less dense environments. However, these environmental differences can not be confirmed at a high significance level from this analysis. The local density may have a role in triggering AGN activity. It would be interesting to explore whether the observed differences in the physical properties of AGN and SFG, as shown in Figure 6, persist in regions of different

https://doi.org/10.1017/pasa.2025.10052 Published online by Cambridge University Press

density. To investigate this, we divide the mass-matched AGN and SFG into two categories based on local density. Galaxies residing in regions with a density below the median of the combined sample are classified as "low density", while those in regions with a density above the median are classified as "high density".

We calculate the PDFs of four galaxy properties for AGN and SFG in both low-density and high-density regions. The comparisons of physical properties for AGN and SFG in low-density regions are shown in the four left panels of Figure 7, while the comparisons in high-density regions are displayed in the four right panels. The differences between the PDFs in each panel are quantified using the KS-test. The results show that the null hypothesis can be rejected with a confidence level greater than 99.99% in all cases, indicating that the differences in the physical properties of AGN and SFG persist in both low- and high-density regions.

AGN activity can be triggered in both high- and low-density environments, and its presence significantly alters the physical properties of the host galaxy compared to those of a SFG. Notably, the differences in physical properties between AGN and SFG persist regardless of local environmental density. This indicates that such differences can not be explained by variations in local density.

4. Conclusion

We use a volume-limited sample from the SDSS to compare the clustering and physical properties of SFG and AGN host galaxies at fixed stellar mass. Our analysis with two-point correlation function and the 5^{th} nearest neigbour distance reveals that the clustering strength of AGN are moderately stronger than SFG. However, the statistical significance of these differences are not sufficiently strong to confirm these environmental differences. The weak significance may arise due to the small size of our samples. Further analysis with larger datasets are required for conclusive evidence.

We further compare the distributions of $(u-r)$ colour, concentration index, SFR, and D4000 for AGN and SFG at fixed stellar mass and find statistically significant differences at a confidence level exceeding 99.99%. These distributions are also examined across varying densities while maintaining fixed stellar mass, revealing that the differences persist at the same significance level in both high and low-density environments (Figure 7). This suggests that the observed differences in the physical properties of AGN and SFG cannot be attributed solely to their local density. Instead, density may play an indirect role in AGN activity by increasing the likelihood of galaxy interactions (Ellison et al., 2011; Sabater, Best, and Heckman, 2015; Singh et al., 2023). In relaxed systems, gas is unable to flow toward the central SMBH due to angular momentum conservation. Interactions can generate torques or instabilities that funnel gas toward the SMBH, thereby triggering AGN activity (Woods and Geller, 2007; Rogers et al., 2009). Although the number density of galaxies in cluster environments is much higher than in the field, the higher velocities of galaxies, particularly those newly infalling near the cluster center, can inhibit interactions. Haines et al. (2012) provide evidence suggesting that galaxy interactions may still play an important role in the cluster outskirts, offering a scenario where such interactions are more likely to occur. Ehlert et al. (2015) suggested that galaxy mergers could play a significant role in contributing to the AGN population within clusters. Several other works Koulouridis, Gkini, and Drigga (2024); Drigga et al. (2025) presented additional evidence in support of this idea. Notably, our results indicate that AGN activity can also be sustained through secular processes in low density environments.

Galaxies with similar stellar masses can exhibit significantly different assembly histories, creating uncertainties about whether a galaxy of a given stellar mass can host the conditions necessary for AGN activity. Two key prerequisites for AGN activity are the presence of a bulge and the availability of gas (Ruffa et al., 2019; Shangguan et al., 2020; Ellison et al., 2021; Sampaio et al., 2023). However, these favorable conditions are met only in a subset of galaxies at a given stellar mass, with their prevalence depending on both stellar mass and assembly history. Studies indicate that the frequency of bulge formation increases with stellar mass (Erwin and Debattista, 2017) and is influenced by assembly history (Kruk et al., 2019). Hydrodynamical simulations further suggest that assembly bias can lead to substantial variations in the cold gas content of galaxies (Cui et al., 2021). For instance, galaxies with higher stellar masses tend to reside in early-formed halos, which are more likely to accumulate large reservoirs of cold gas. Consequently, the availability of cold gas is governed by both stellar mass and the assembly history of the host halos.

The observed increase in AGN fraction with stellar mass is linked to the greater likelihood of bulge dominance and the presence of larger cold gas reservoirs in more massive galaxies. Additionally, massive halos, which reside in denser environments, are subject to more frequent interactions. These interactions can influence AGN activity and may be reflected in the clustering properties of galaxies. Croton, Gao, and White (2007) demonstrate that assembly bias alters the two-point correlation function of galaxies by $\sim 10\%$. It would be difficult to confirm the role of assembly bias from such small differences in the observed two-point correlation functions. Using information theoretic measures, several studies show that galaxy morphology and colour are significantly impacted by large-scale environment (Pandey and Sarkar, 2017; Sarkar and Pandey, 2020; Sarkar, Pandey, and Das, 2022). Such dependence hints towards possible roles of assembly bias in shaping the galaxy properties. We plan to compare the large-scale environment of SFG and AGN in future work.

Massive galaxies predominantly inhabit denser environments, and AGN hosts are typically high-mass galaxies. Since galaxy clustering is strongly influenced by mass, our SFG and AGN samples are matched in stellar mass. AGN exhibit only a moderately stronger clustering than SFG, suggesting that local density may not have a significant role in triggering AGN activity. Further, the observed differences in the physical properties of mass-matched SFG and AGN remain largely independent of environmental density. This also indicates that the local environment is unlikely to be the primary driver of AGN activity.

Our findings hint at a potential role of assembly history in influencing AGN activity. However, the current analysis does not provide conclusive evidence, necessitating further investigation. The relationship between assembly bias and AGN activity is inherently complex, involving an intricate interplay between the formation histories of galaxies, the properties of their host dark matter halos, and the mechanisms that trigger and regulate AGN activity. A deeper understanding of these connections is essential to uncover the influence of assembly bias on AGN activity. We plan to use hydrodynamical simulations, such as EAGLE (Schaye et al., 2015) and IllustrisTNG (Nelson et al., 2019) in future work, to explore these aspects in greater detail.

https://doi.org/10.1017/pasa.2025.10052 Published online by Cambridge University Press

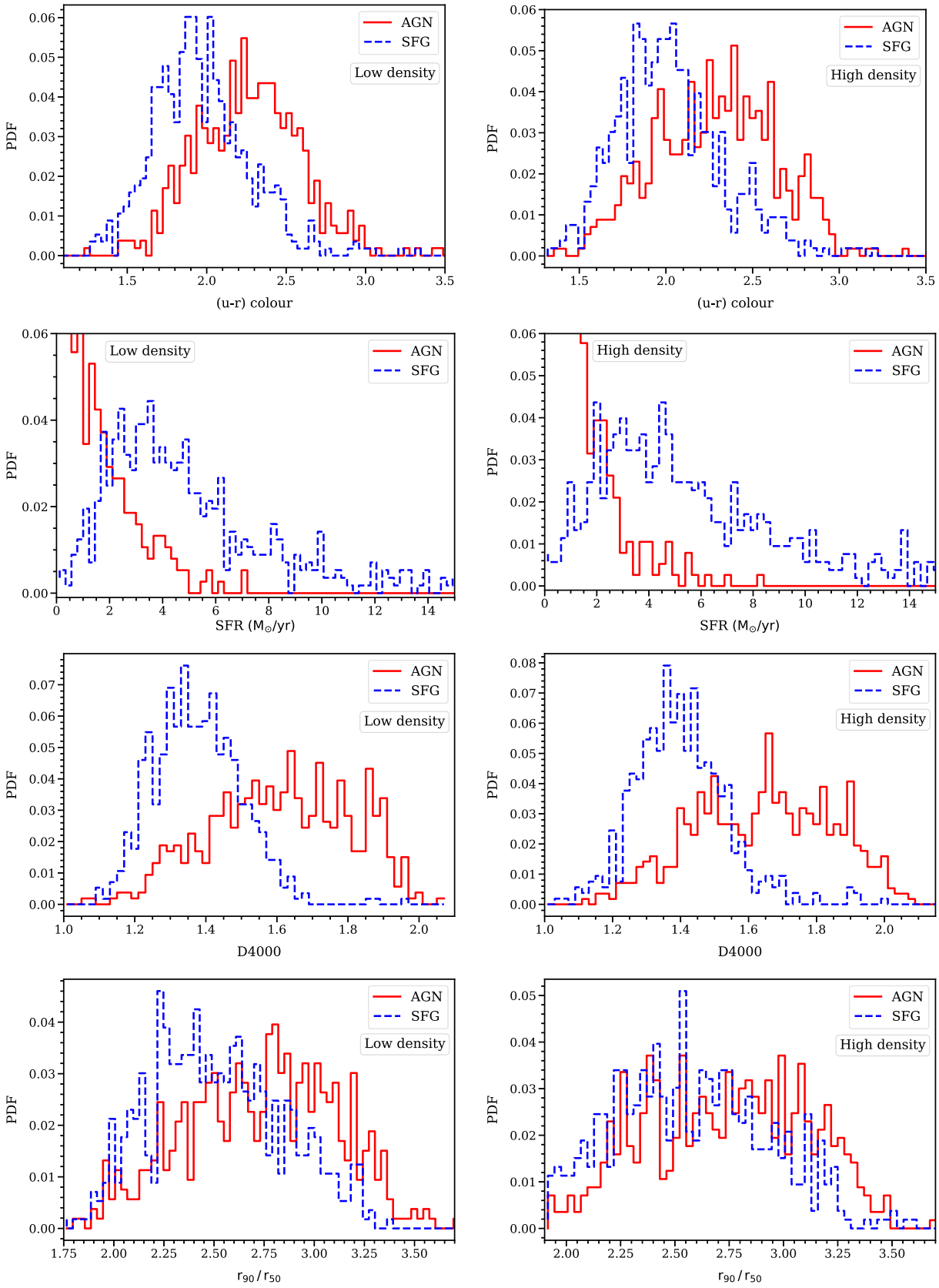

Figure 7. The four left panels of this figure show the PDFs of $(u-r)$ colour, SFR, D4000 and $\frac{r_{90}}{r_{50}}$ for the mass-matched AGN and SFG in the low density regions. The four right panels show the same in the high density regions. The KS test shows that the null hypothesis can be rejected at $>$ 99.99% confidence level in each case.

https://doi.org/10.1017/pasa.2025.10052 Published online by Cambridge University Press

Acknowledgement. The authors thank an anonymous reviewer and the associate editor for the valuable comments and suggestions that helped to improve the draft. BP would like to acknowledge financial support from the SERB, DST, Government of India through the project CRG/2019/001110. BP would also like to acknowledge IUCAA, Pune, for providing support through the associateship programme. AN acknowledges the financial support from the Department of Science and Technology (DST), Government of India through an INSPIRE fellowship. The authors thank Tapas Kumar Das for some interesting discussions.

Funding for the SDSS and SDSS-II has been provided by the Alfred P. Sloan Foundation, the Participating Institutions, the National Science Foundation, the U.S. Department of Energy, the National Aeronautics and Space Administration, the Japanese Monbukagakusho, the Max Planck Society, and the Higher Education Funding Council for England. The SDSS website is https://www.sdss.org/.

The SDSS is managed by the Astrophysical Research Consortium for the Participating Institutions. The Participating Institutions are the American Museum of Natural History, Astrophysical Institute Potsdam, University of Basel, University of Cambridge, Case Western Reserve University, University of Chicago, Drexel University, Fermilab, the Institute for Advanced Study, the Japan Participation Group, Johns Hopkins University, the Joint Institute for Nuclear Astrophysics, the Kavli Institute for Particle Astrophysics and Cosmology, the Korean Scientist Group, the Chinese Academy of Sciences (LAMOST), Los Alamos National Laboratory, the Max-Planck-Institute for Astronomy (MPIA), the Max-Planck-Institute for Astrophysics (MPA), New Mexico State University, Ohio State University, University of Pittsburgh, University of Portsmouth, Princeton University, the United States Naval Observatory, and the University of Washington.

Data availability statement. The SDSS data are publicly available at https://skyserver.sdss.org/casjobs/. The data generated in this work will be shared on reasonable request to the authors.

References

Abadi, M. G., Moore, B., & Bower, R. G. 1999, MNRAS, 308, 947
Abdurro'uf, K. A., Aerts, C., Aguirre, V. S., Ahumada, R., Ajgaonkar, N., Ak, N. F., et al. 2022, ApJS, 259, 35
Aird, J., & Coil, A. L. 2021, MNRAS, 502, 5962
Alexander, D. M., & Hickox, R. C. 2012, New A Rev., 56, 93
Alonso, M. S., Lambas, D. G., Tissera, P., & Coldwell, G. 2007, MNRAS, 375, 1017
Alonso, S., Coldwell, G., & Lambas, D. G. 2014, A&A, 572, A86
Amiri, A., Tavasoli, S., & De Zotti, G. 2019, ApJ, 874, 140
Antonuccio-Delogu, V., & Silk, J. 2010, MNRAS, 405, 1303
Baldry, I. K., Glazebrook, K., Brinkmann, J., Ivezic, Ž., Lupton, R. H., Nichol, R. C., & Szalay, A. S. 2004, ApJ, 600, 681
Balogh, M. L., Baldry, I. K., Nichol, R., Miller, C., Bower, R., & Glazebrook, K. 2004, ApJ, 615, L101
Balogh, M. L., Morris, S. L., Yee, H. K. C., Carlberg, R. G., & Ellingson, E. 1999, ApJ, 527, 54
Baron, D., Netzer, H., Prochaska, J. X., Cai, Z., Cantalupo, S., Martin, D. C., Matuszewski, M., Moore, A. M., Morrissey, P., & Neill, J. D. 2018, MNRAS, 480, 3993
Behroozi, P. S., Wechsler, R. H., & Conroy, C. 2013, ApJ, 770, 57
Birnboim, Y., & Dekel, A. 2003, MNRAS, 345, 349
Blanton, M. R., Dalcanton, J., Eisenstein, D., Loveday, J., Strauss, M. A., SubbaRao, M., Weinberg, D. H., et al. 2001, AJ, 121, 2358
Blanton, M. R., Hogg, D. W., Bahcall, N. A., Baldry, I. K., Brinkmann, J., Csabai, I., Eisenstein, D., et al. 2003, ApJ, 594, 186
Boselli, A., Fossati, M., & Sun, M. 2022, A&A Rev., 30, 3
Bradshaw, E. J., Almaini, O., Hartley, W. G., Chuter, R. W., Simpson, C., Conselice, C. J., Dunlop, J. S., McLure, R. J., & Cirasuolo, M. 2011, MNRAS, 415, 2626
Brinchmann, J., Charlot, S., White, S. D. M., Tremonti, C., Kauffmann, G., Heckman, T., & Brinkmann, J. 2004, MNRAS, 351, 1151
Brusa, M., Fiore, F., Santini, P., Grazian, A., Comastri, A., Zamorani, G., Hasinger, G., et al. 2009, A&A, 507, 1277
Bruton, S. T., Dai, X., Guerras, E., & Munshi, F. A. 2020, MNRAS, 491, 2496
Bufanda, E., Hollowood, D., Jeltema, T. E., Rykoff, E. S., Rozo, E., Martini, P., Abbott, T. M. C., et al. 2017, MNRAS, 465, 2531
Casertano, S., & Hut, P. 1985, ApJ, 298, 80–94
Ceccarelli, L., Duplancic, F., & Lambas, D. G. 2021, arXiv e-prints (November): arXiv:2111.11488. https://doi.org/10.48550/arXiv.2111.11488
Choi, Y.-Y., Woo, J.-H., & Park, C. 2009, ApJ, 699, 1679
Cielo, S., Bieri, R., Volonteri, M., Wagner, A. Y., & Dubois, Y. 2018, MNRAS, 477, 1336
Cimatti, A., Brusa, M., Talia, M., Mignoli, M., Rodighiero, G., Kurk, J., Cassata, P., Halliday, C., Renzini, A., & Daddi, E. 2013, ApJ, 779, L13
Constantin, A., Hoyle, F., & Vogeley, M. S. 2008, ApJ, 673, 715
Cooray, A., & Sheth, R. 2002, PhR, 372, 1
Croton, D. J., Gao, L., & White, S. D. M. 2007, MNRAS, 374, 1303
Cui, W., Davé, R., Peacock, J. A., Anglés-Alcázar, D., & Yang, X. 2021, NatAs, 5, 1069
Das, A., Pandey, B., & Sarkar, S. 2023a, RAA, 23, 095026
Das, A., Pandey, B., & Sarkar, S. 2023b, RAA, 23, 025016
Das, A., Pandey, B. & Sarkar, S. 2023c, arXiv e-prints: arXiv:2303.16826. https://doi.org/10.48550/arXiv.2303.16826
Dekel, A., & Birnboim, Y. 2006, MNRAS, 368, 2
Dekel, A., Sari, R., & Ceverino, D. 2009, ApJ, 703, 785
Di Matteo, T., Springel, V., & Hernquist, L. 2005, Nature 433, 604
Donoso, E., Yan, L., Stern, D., & Assef, R. J. 2014, ApJ, 789, 44
Drigga, E., Koulouridis, E., Pouliasis, E., Toba, Y., Akiyama, M., Vignali, C., Georgantopoulos, I., et al. 2025, arXiv e-prints: arXiv:2504.03422. https://doi.org/10.48550/arXiv.2504.03422.
Dunlop, J. S., McLure, R. J., Kukula, M. J., Baum, S. A., O'Dea, C. P., & Hughes, D. H. 2003, MNRAS, 340, 1095
Eckert, D., Gaspari, M., Gastaldello, F., Le Brun, A. M. C., & O'Sullivan, E. 2021, Universe, 7, 142
Ehlert, S., Allen, S. W., Brandt, W. N., Canning, R. E. A., Luo, B., Mantz, A., Morris, R. G., von der Linden, A., & Xue, Y. Q. 2015, MNRAS, 446, 2709
Ehlert, S., von der Linden, A., Allen, S. W., Brandt, W. N., Xue, Y. Q., Luo, B., Mantz, A., Morris, R. G., Applegate, D., & Kelly, P. 2014, MNRAS, 437, 1942
Ellison, S. L., Patton, D. R., Mendel, J. T., & Scudder, J. M. 2011, MNRAS, 418, 2043
Ellison, S. L., Wong, T., Sánchez, S. F., Colombo, D., Bolatto, A., Barrera-Ballesteros, J., Garca-Benito, R., et al. 2021, MNRAS, 505, L46
Erwin, P., & Debattista, V. P. 2017, MNRAS, 468, 2058
Fabian, A. C. 1999, PNAS, 96, 4749
Fabian, A. C. 2012, ARA&A, 50, 455
Fassbender, R., Šuhada, R., & Nastasi, A. 2012, AdAst, 2012, 138380
Gabor, J. M., Davé, R., Finlator, K., & Oppenheimer, B. D. 2010, MNRAS, 407, 749
Gao, L., Springel, V., & White, S. D. M. 2005, MNRAS, 363, L66
Gao, L., & White, S. D. M. 2007, MNRAS, 377, L5
Gatica, C., Demarco, R., Dole, H., Polletta, M., Frye, B., Martinache, C., & Rettura, A. 2024, MNRAS, 527, 3006
Georgakakis, A., Comparat, J., Merloni, A., Ciesla, L., Aird, J., & Finoguenov, A. 2019, MNRAS, 487, 275
Gilli, R., Zamorani, G., Miyaji, T., Silverman, J., Brusa, M., Mainieri, V., Cappelluti, N., et al. 2009, A&A, 494, 33
Gilmour, R., Gray, M. E., Almaini, O., Best, P., Wolf, C., Meisenheimer, K., Papovich, C., & Bell, E. 2007, MNRAS, 380, 1467
Grogin, N. A., and Geller, M. J. 2000, AJ, 119, 32
Gunn, J. E., and Richard III, G. J. 1972, ApJ, 176, 1
Gunn, J. E., Siegmund, W. A., Mannery, E. J., Owen, R. E., Hull, C. L., Leger, R. F., Carey, L. N., et al. 2006, AJ, 131, 2332
Haines, C. P., Pereira, M. J., Sanderson, A. J. R., Smith, G. P., Egami, E., Babul, A., Edge, A. C., Finoguenov, A., Moran, S. M., & Okabe, N. 2012, ApJ, 754, 97
Hale, C. L., Jarvis, M. J., Delvecchio, I., Hatfield, P. W., Novak, M., Smolcic, V., & Zamorani, G. 2018, MNRAS, 474, 4133
Harrison, C. M. 2017, NatAs, 1, 0165

Hashiguchi, A., Toba, Y., Ota, N., Oguri, M., Okabe, N., Ueda, Y., Imanishi, M., et al. 2023, PASJ, 75, 1246
Hasinger, G. 2008. A&A, 490, 905
Hawkins, E., Maddox, S., Cole, S., Lahav, O., Madgwick, D. S., Norberg, P., Peacock, J. A., et al. 2003, MNRAS, 346, 78
Heckman, T. M., & Best, P. N. 2014, ARA&A, 52, 589–660
Hernquist, L. 1989, Nature, 340, 687
Hopkins, A. M. 2004, ApJ, 615, 209
Hopkins, P. F., & Hernquist, L. 2006, ApJS, 166, 1
Hopkins, P. F., Kocevski, D. D., & Bundy, K. 2014, MNRAS, 445, 823
Hoyle, F., Rojas, R. R., Vogeley, M. S., & Brinkmann, J. 2005, ApJ, 620, 618
Jiang, Y.-F., Stone, J. M., & Davis, S. W. 2013, ApJ, 778, 65
Kauffmann, G., & Heckman, T. M. 2009, MNRAS, 397, 135
Kauffmann, G., Heckman, T. M., Tremonti, C., Brinchmann, J., Charlot, S., White, S. D. M., Ridgway, S. E., et al. 2003, MNRAS, 346, 1055
Kauffmann, G., Heckman, T. M., White, S. D. M., Charlot, S., Tremonti, C., Peng, E. W., Seibert, M., et al. 2003, MNRAS, 341, 54
Kauffmann, G., White, S. D. M., Heckman, T. M., Ménard, B., Brinchmann, J., Charlot, S., Tremonti, C., & Brinkmann, J. 2004, MNRAS, 353, 713
Kawata, D., & Gibson, B. K. 2005, MNRAS, 358, L16
Kereš, D., Katz, N., Weinberg, D. H., & Davé, R. 2005, MNRAS, 363, 2
Kollatschny, W., Reichstein, A., & Zetzl, M. 2012, A&A, 548, A37
Kormendy, J., & Ho, L. C. 2013, ARA&A, 51, 511
Koulouridis, E., Gkini, A., & Drigga, E. 2024, A&A, 684, A111
Koulouridis, E., Ricci, M., Giles, P., Adami, C., Ramos-Ceja, M., Pierre, M., Plionis, M., et al. 2018, A&A, 620, A20
Krishnan, C., Hatch, N. A., Almaini, O., Kocevski, D., Cooke, E. A., Hartley, W. G., Hasinger, G., Maltby, D. T., Muldrew, S. I., & Simpson, C. 2017, MNRAS, 470, 2170
Kruk, S. J., Erwin, P., Debattista, V. P., & Lintott, C. 2019, MNRAS, 490, 4721
Lacerna, I., Hernández-Toledo, H. M., Avila-Reese, V., Abonza-Sane, J., & del Olmo, A. 2016, A&A, 588, A79
Landy, S. D., & Szalay, A. S. 1993, ApJ, 412, 64
Larson, R. B., Tinsley, B. M., & Caldwell, C. N. 1980, ApJ, 237, 692
Lee, J., Shin, J., Snaith, O. N., Kim, Y., Few, C. G., Devriendt, J., Dubois, Y., et al. 2021, ApJ, 908, 11
Lehmer, B. D., Lucy, A. B., Alexander, D. M., Best, P. N., Geach, J. E., Harrison, C. M., Hornschemeier, A. E., et al. 2013, ApJ, 765, 87
Lopes, P. A. A., Ribeiro, A. L. B., & Rembold, S. B. 2017, MNRAS, 472, 409
Luo, W., Silverman, J. D., More, S., Goulding, A., Miyatake, H., Nishimichi, T., Hikage, C., et al. 2022, arXiv e-prints: arXiv:2204.03817. https://doi.org/10.48550/arXiv.2204.03817
Madau, P., Ferguson, H. C., Dickinson, M. E., Giavalisco, M., Steidel, C. C., & Fruchter, A. 1996, MNRAS, 283, 1388
Man, Z.-y., Peng, Y.-j., Kong, X., Guo, K.-x., Zhang, C.-p., & Dou, J. 2019, MNRAS, 488, 89
Mandelbaum, R., Li, C., Kauffmann, G., & White, S. D. M. 2009, MNRAS, 393, 377
Martini, P., Miller, E. D., Brodwin, M., Stanford, S. A., Gonzalez, A. H., Bautz, M., Hickox, R. C., et al. 2013, ApJ, 768, 1
Martini, P., Mulchaey, J. S., & Kelson, D. D. 2007, ApJ, 664, 761
McNamara, B. R., & Nulsen, P. E. J. 2012, New Journal of Physics, 14, 055023
Miller, C. J., Nichol, R. C., Gómez, P. L., Hopkins, A. M., & Bernardi, M. 2003, ApJ, 597, 142
Miraghaei, H. 2020, AJ, 160, 227
Mishra, H. D., & Dai, X. 2020, AJ, 159, 69
Mishra, H. D., Dai, X., & Guerras, E. 2021, ApJ, 922, L17
Moore, B., Katz, N., Lake, G., Dressler, A., & Oemler, A. 1996, Nature, 379, 613
Morganti, R. 2017, Front. Astronom. Space Sci., 4, 42
Nandra, K., Georgakakis, A., Willmer, C. N. A., Cooper, M. C., Croton, D. J., Davis, M., Faber, S. M., Koo, D. C., Laird, E. S., & Newman, J. A. 2007, ApJ, 660, L11
Nelson, D., Springel, V., Pillepich, A., Rodriguez-Gomez, V., Torrey, P., Genel, S., Vogelsberger, M., et al. 2019, Computat. Astrophys. Cosmol., 6, 2
Pandey, B. 2020, MNRAS, 499, L31
Pandey, B., & Bharadwaj, S. 2008, MNRAS, 387, 767
Pandey, B., & Sarkar, S. 2017, MNRAS, 467, L6
Pandey, B., & Sarkar, S. 2020, MNRAS, 498, 6069
Peng, Y., Maiolino, R., & Cochrane, R. 2015, Nature, 521, 192
Pierre, M., Pacaud, F., Adami, C., Alis, S., Altieri, B., Baran, N., Benoist, C., et al. 2016, A&A, 592, A1
Pimbblet, K. A., Shabala, S. S., Haines, C. P., Fraser-McKelvie, A., & Floyd, D. J. E. 2013, MNRAS, 429, 1827
Planck Collaboration, Aghanim, N., Akrami, Y., Ashdown, M., Aumont, J., Baccigalupi, C., Ballardini, M., et al. 2020, A&A, 641, A6
Porqueres, N., Jasche, J., Enßlin, T. A., & Lavaux, G. 2018, A&A, 612, A31
Ricciardelli, E., Cava, A., Varela, J., & Quilis, V. 2014, MNRAS, 445, 4045
Rogers, B., Ferreras, I., Kaviraj, S., Pasquali, A., & Sarzi, M. 2009, MNRAS, 399, 2172
Ruffa, I., Davis, T. A., Prandoni, I., Laing, R. A., Paladino, R., Parma, P., de Ruiter, H., Casasola, V., Bureau, M., & Warren, J. 2019, MNRAS, 489, 3739–3757
Sabater, J., Best, P. N., & Argudo-Fernández, M. 2013, MNRAS, 430, 638
Sabater, J., Best, P. N., & Heckman, T. M. 2015, MNRAS, 447, 110
Salim, S., Rich, R. M., Charlot, S., Brinchmann, J., Johnson, B. D., Schiminovich, D., Seibert, M., et al. 2007, ApJS, 173, 267
Sampaio, V. M., Aragón-Salamanca, A., Merrifield, M. R., de Carvalho, R. R., Zhou, S., & Ferreras, I. 2023, MNRAS, 524, 5327
Santoro, F., Tadhunter, C., Baron, D., Morganti, R., & Holt, J. 2020, A&A, 644, A54
Sarkar, S., & Pandey, B. 2020, MNRAS, 497, 4077
Sarkar, S., Pandey, B., & Das, A. 2022, J. Cosmol. Astropart. Phys., 2022, 024
Satyapal, S., Ellison, S. L., McAlpine, W., Hickox, R. C., Patton, D. R., & Mendel, J. T. 2014, MNRAS, 441, 1297
Schaye, J., Crain, R. A., Bower, R. G., Furlong, M., Schaller, M., Theuns, T., Vecchia, C. D., et al. 2015, MNRAS, 446, 521
Shangguan, J., Ho, L. C., Bauer, F. E., Wang, R., & Treister, E. 2020, ApJ, 899, 112
Shimasaku, K., Fukugita, M., Doi, M., Hamabe, M., Ichikawa, T., Okamura, S., Sekiguchi, M., et al. 2001, AJ, 122, 1238
Silverman, J. D., Kovac, K., Knobel, C., Lilly, S., Bolzonella, M., Lamareille, F., Mainieri, V., et al. 2009, ApJ, 695, 171
Silverman, J. D., Mainieri, V., Lehmer, B. D., Alexander, D. M., Bauer, F. E., Bergeron, J., Brandt, W. N., et al. 2008, ApJ, 675, 1025
Singh, A., Park, C., Choi, E., Kim, J., Jun, H., Gibson, B. K., Kim, Y., Lee, J., & Snaith, O. 2023, ApJ, 953, 64
Sinha, M., & Garrison, L. H. 2020, MNRAS, 491, 3022
Somerville, R. S., Hopkins, P. F., Cox, T. J., Robertson, B. E., & Hernquist, L. 2008, MNRAS, 391, 481
Springel, V., Di Matteo, T., & Hernquist, L. 2005, MNRAS, 361, 776
Storchi-Bergmann, T., & Schnorr-Müller, A. 2019, NatAs, 3, 48
Stoughton, C., Lupton, R. H., Bernardi, M., Blanton, M. R., Burles, S., Castander, F. J., Connolly, A. J., et al. 2002, AJ, 123, 485
Strateva, I., Ivezic, Ž., Knapp, G. R., Narayanan, V. K., Strauss, M. A., Gunn, J. E., Lupton, R. H., et al. 2001, AJ, 122, 1861
Strauss, M. A., Weinberg, D. H., Lupton, R. H., Narayanan, V. K., Annis, J., Bernardi, M., Blanton, M., et al. 2002, AJ, 124, 1810
Umehata, H., Fumagalli, M., Smail, I., Matsuda, Y., Swinbank, A. M., Cantalupo, S., Sykes, C., et al. 2019, Science, 366, 97
Vito, F., Brandt, W. N., Comastri, A., Gilli, R., Ivison, R. J., Lanzuisi, G., Lehmer, B. D., Lopez, I. E., Tozzi, P., & Vignali, C. 2024, A&A, 689, A130
Wagner, A. Y., Umemura, M., & Bicknell, G. V. 2013, ApJ, 763, L18
Wang, L., & Li, C. 2019, MNRAS, 483, 1452
Wechsler, R. H., Zentner, A. R., Bullock, J. S., Kravtsov, A. V., & Allgood, B. 2006, ApJ, 652, 71
Woo, J.-H., & Urry, C. M. 2002, ApJ, 579, 530
Woods, D. F., & Geller, M. J. 2007, AJ, 134, 527
Zezas, A., Hernquist, L., Fabbiano, G., & Miller, J. 2003, ApJ, 599, L73
Zhang, Z., Wang, H., Luo, W., Mo, H. J., Liang, Z., Li, R., Yang, X., et al. 2021, A&A, 650, A155

https://doi.org/10.1017/pasa.2025.10052 Published online by Cambridge University Press